

# Lawrence Berkeley National Laboratory

## LBL Publications

### Title

Remote Off-grid Microgrid Design Support Tool (ROMDST) - An Optimal Design Support Tool for Remote, Resilient, and Reliable Microgrids Phase II - Final Report

### Permalink

<https://escholarship.org/uc/item/1rj9s7g3>

### Authors

Cardoso, Goncalo  
Heleno, Miguel  
DeForest, Nicholas

### Publication Date

2019-03-05

### DOI

10.2172/1506410

Peer reviewed



LBNL 0000

# Lawrence Berkeley National Laboratory

## **Remote Off-grid Microgrid Design Support Tool (ROMDST) - An Optimal Design Support Tool for Remote, Resilient, and Reliable Microgrids**

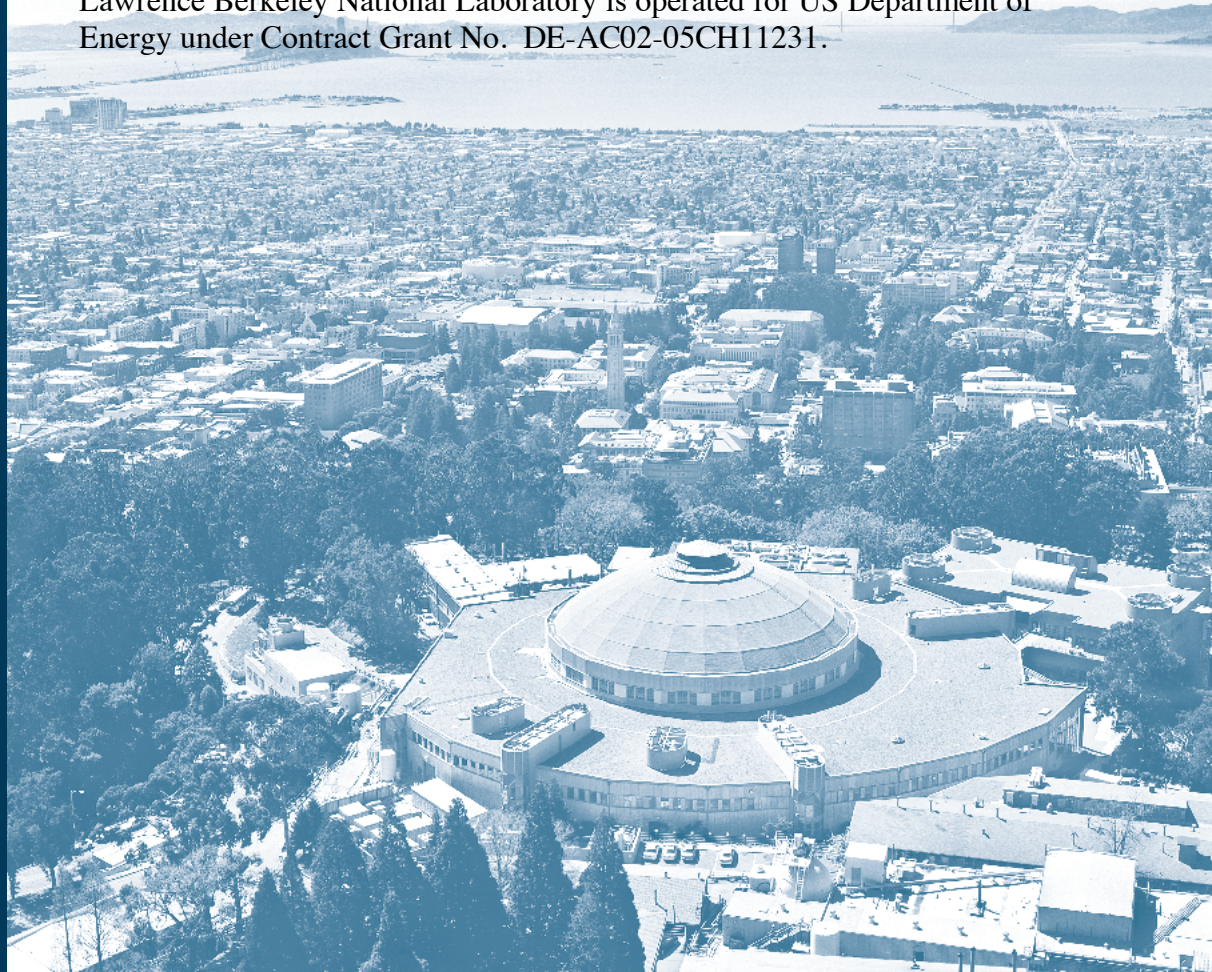
### **Phase II – Final Report**

G. Cardoso, M. Heleno, N. DeForest

**Grid Integration Group, Lawrence Berkeley National Laboratory**

July, 2018

Lawrence Berkeley National Laboratory is operated for US Department of Energy under Contract Grant No. DE-AC02-05CH11231.



## **Disclaimer**

This document was prepared as an account of work sponsored by the United States Government. While this document is believed to contain correct information, neither the United States Government nor any agency thereof, nor The Regents of the University of California, nor any of their employees, makes any warranty, express or implied, or assumes any legal responsibility for the accuracy, completeness, or usefulness of any information, apparatus, product, or process disclosed, or represents that its use would not infringe privately owned rights. Reference herein to any specific commercial product, process, or service by its trade name, trademark, manufacturer, or otherwise, does not necessarily constitute or imply its endorsement, recommendation, or favoring by the United States Government or any agency thereof, or The Regents of the University of California. The views and opinions of authors expressed herein do not necessarily state or reflect those of the United States Government or any agency thereof or The Regents of the University of California.

# ROMDST - An Optimal Design Support Tool for Remote, Resilient, and Reliable Microgrids

## Phase II – Final Report

July 2018

Gonçalo Cardoso, Miguel Heleno, Nicholas DeForest

Lawrence Berkeley National Lab

Project Partners







## Table of Contents

- 1 Introduction..... 4
- 2 Summary of Phase II accomplishments ..... 6
- 3 Discussion of Phase II accomplishments..... 7
  - 3.1 Component Library Development..... 7
    - 3.1.1 Data collection: microgrid device ..... 7
    - 3.1.2 Data collection: grid components ..... 8
    - 3.1.3 Component library update..... 9
  - 3.2 Optimization formulation and Numeric Implementation ..... 10
    - 3.2.1 Stochastic generation formulation..... 10
    - 3.2.2 Chance constrained formulation and implementation ..... 11
    - 3.2.3 Network design formulation and implementation..... 12
  - 3.3 Network Design and Visualization..... 14
    - 3.3.1 GIS Visualization ..... 14
  - 3.4 Design/Dispatch sensitivity calculations..... 15
    - 3.4.1 Design sensitivity..... 15
  - 3.5 Tool Testing..... 16
    - 3.5.1 Testing against current microgrids – tech mix and operation ..... 16
    - 3.5.2 Testing against existing design tools ..... 17
    - 3.5.3 Verification against power flow software..... 20
  - 3.6 Transition to end users..... 22
    - 3.6.1 Manual preparation..... 22
    - 3.6.2 Holding training classes ..... 23
- 4 Annex – Details on Formulation and Testing ..... 27
  - 4.1 Details on chance constrained formulation..... 27
  - 4.2 Details on microgrid testing..... 31



U.S. DEPARTMENT OF  
**ENERGY**

**DER-CAM+** DECISION SUPPORT TOOL FOR  
DECENTRALIZED ENERGY SYSTEMS  
TOPOLOGY | ANALYTICS | PLANNING | OPERATIONS



## 1 Introduction

The objective of the project is to develop an advanced optimization-based design support tool for AC or DC microgrids in remote locations, where utility grids may not be accessible. The mathematical model and the interface are being developed such that multiple design objectives and criteria/constraints can be easily enabled or disabled, to deliver a flexible tool relevant to a large, diverse user base, and to facilitate future feature developments.

The new tool delivered by this project leverages the team's extensive expertise in the development, testing, deployment, and commercialization of the state-of-the-art Distributed Energy Resources Customer Adoption Model (DER-CAM) – which is the foundation for the new tool. This project has been structured in two phases, each originally planned to last 10 months.

Phase I leveraged heavily on DER-CAM. This state-of-the-art tool has been applied to microgrid design and analysis problems by many prestigious industry names including EPRI, GE, and Burns Engineering, and several NY Prize winners use it for microgrid design studies. Key Phase I developments included adapting DER-CAM model to meet the requirements of this project, including: a) AC or DC microgrid architectures, b) multiple economic objectives (e.g. single customer vs community vs utility perspective), c) constraints on fuel availability (e.g. total fuel available during outage periods), d) active and reactive power flow constraints for normal and N-1 contingency cases, e) component part load efficiencies (e.g. power electronic devices), and f) interactive data visualization capabilities (e.g. design topology elements). A component library including components' default technical and economical characteristics was also developed. In Phase II, the project is focused on tool testing and validation, use for real-world microgrid designs, and outreach. This phase also includes tasks for further enhance the model by expanding the component library, developing a formulation to address stochasticity in renewable generation, adding network design capabilities, enhancing the visualization and interface, and enhancing the computational performance.

To carry out the project, a team of several national labs, industrial partners, and microgrid governing entities has been formed. Lawrence Berkeley National Lab (LBNL), Los Alamos National Lab (LANL), and Argonne National Lab (ANL), with extensive experience in microgrid design, modeling, and optimization, are jointly developing the tool. Brookhaven National Laboratory (BNL), Burns Engineering, and General Electric's Energy Consulting group are focusing on testing and validation of the tool using data from real microgrids. Through these efforts, the ROMDST project is delivering a tested and verified optimal design tool for remote, resilient, and reliable microgrids, and the relevant supporting materials. Fully developing this tool will have the following impacts: 1) optimal off-grid microgrid designs that replace existing back of the envelope or non-optimal calculations, reducing capital costs and risk of microgrid deployment; 2) removing barriers to microgrid assessments by lowering microgrid soft costs, as the tool



is freely usable; 3) reliable and resilient designs that reduce the cost of critical load shedding due to component outages.

The new tool has been developed on the existing foundation of DER-CAM. The significance and impact of DER-CAM and this project has also been recognized in multiple occasions, including the Presidential Early Career Award for Scientists and Engineers (May 2016), and the selection as a finalist for the 2016 R&D 100 awards, along with a continuously growing user base and inclusion in high-impact initiatives such as the NY PRIZE, where DER-CAM was the tool of choice in a large number of applications.

This report reviews what was achieved during Phase II of the project.

Further, advancements made to the tool's optimization formulation and details about the planned case studies are included in the appendices.



## 2 Summary of Phase II accomplishments

The Phase II work planned for this project was organized around 7 core tasks. These tasks include 1) the development of a component library to facilitate the creation of new models using pre-processed datasets; 2) exploring and developing enhanced optimization formulations to account for uncertainty and allow network design to be included in the optimization process; 3) carry out the numeric implementation of the enhanced formulations; 4) extend the user interface to accommodate additional design and visualization capabilities; 5) develop new sensitivity analysis capabilities to enable flexible studies; 6) carry out tool testing and validation; 7) transition the tool to users and conduct outreach.

These tasks were arranged according to the timeline presented in Table 1. This reflects adjustments both in duration to 12 months and May 2017 start, as approved by DOE.

Table 1 Summary of phase II timeline

	Phase II Months											
	5-17	6-17	7-17	8-17	9-17	10-17	11-17	12-17	1-18	2-18	3-18	4-18
	1	2	3	4	5	6	7	8	9	10	11	12
<b>Task 1: Component library development</b>	[Task 1 bar]											
Task 1.1: Data collection: microgrid device	[Task 1.1 bar]											
Task 1.2: Data collection: grid components	[Task 1.2 bar]											
Task 1.3: Component library update						M5						
Task 1.4: Local dispatch characterization												
<b>Task 2: Optimization formulation</b>	[Task 2 bar]											
Task 2.1: Stochastic generation modeling	[Task 2.1 bar]											
Task 2.2: Chance constraints formulation	[Task 2.2 bar]											
Task 2.3: Network design formulation	[Task 2.3 bar]											
<b>Task 3: Numerical implementation</b>	[Task 3 bar]											
Task 3.1: Implement chance constraints						M6						
Task 3.2: Network Design									M7			
<b>Task 4: Network design and visualization</b>	[Task 4 bar]											
Task 4.1: GIS visualization	[Task 4.1 bar]											
<b>Task 5: Design/Dispatch sensitivity calculations</b>	[Task 5 bar]											
Task 5.1: Design sensitivity												
<b>Task 6: Tool testing</b>	[Task 6 bar]											
Task 6.1: Testing against current microgrids - tech mix	[Task 6.1 bar]											
Task 6.2: Testing against current microgrids - operation	[Task 6.2 bar]											
Task 6.3: Testing against existing design tools	[Task 6.3 bar]											
Task 6.4: Tool verification against power flow software	[Task 6.4 bar]											
<b>Task 7: Transition to end users</b>	[Task 7 bar]											
Task 7.1: Manual preparation												M8
Task 7.2: Holding training classes												M8
Task 7.3: Tool adoption by a remote community												M8
Task 7.3: Collaborate with microgrid designers												M8

M5, month 4: Final AC/DC microgrid component library is complete  
M6, month 5: Chance constrained optimization formulation (or similar stochastic method) is implemented  
M7, Month 8: Software implementation of the phase II design tool is complete and ready for use in phase II design demonstration  
M8, month 10: End user training and testing is complete; Preparation and submission of the final deliverables is complete



### 3 Discussion of Phase II accomplishments

This section briefly presents project accomplishments in Phase II, following the project task structure.

#### 3.1 Component Library Development

##### 3.1.1 Data collection: microgrid device

**Benefit:** The microgrid device data to be included in the component library allows users to quickly construct models from pre-existing technology definition values without having to conduct extensive data collection.

**Description:** The microgrid device data collection gathers values used in the component library to define technology models as required by the optimization. These values have been collected from industry sources and have been selected to be representative of current technologies, including renewable and fossil-fired generation technologies, storage technologies, CHP technologies, and power electronic converters. A summary of the collected microgrid device data can be found in Table 2.

*Table 2 - Summary of Microgrid Component Parameters*

Technology	Economic Parameters	Operational Parameters
<b>PV Installation</b>	<ul style="list-style-type: none"> <li>Fixed capital cost</li> <li>Power-dependent capital cost</li> <li>Operating cost</li> </ul>	<ul style="list-style-type: none"> <li>Power as a function of irradiance &amp; temperature</li> </ul>
<b>Battery Energy Storage Installation</b>	<ul style="list-style-type: none"> <li>Fixed capital cost</li> <li>Power-dependent capital cost</li> <li>Energy-dependent capital cost</li> <li>Operating cost</li> </ul>	<ul style="list-style-type: none"> <li>Standby loss</li> <li>Maximum battery charge rate</li> <li>Round-trip efficiency curve</li> </ul>
<b>PV Installation with Built-in Battery Energy Storage</b>	<ul style="list-style-type: none"> <li>Fixed capital cost</li> <li>PV power-dependent capital cost</li> <li>Power-dependent capital cost</li> <li>Energy-dependent capital cost</li> <li>Operating cost</li> </ul>	<ul style="list-style-type: none"> <li>Power as a function of irradiance &amp; temperature</li> <li>Efficiency as a function of loading (power) and input/output voltages</li> <li>Standby loss</li> <li>Maximum battery charge rate</li> <li>Round-trip efficiency curve</li> </ul>
<b>Wind Generation Systems</b>	<ul style="list-style-type: none"> <li>Unit capital cost</li> </ul>	<ul style="list-style-type: none"> <li>Power as a function of wind speed</li> <li>Minimum and maximum operating wind speeds</li> <li>Power rating</li> </ul>
<b>Hydro Power Plants</b>	<ul style="list-style-type: none"> <li>Unit capital cost</li> <li>Operating cost</li> </ul>	<ul style="list-style-type: none"> <li>Part-load efficiency curve</li> <li>Maximum ramp rate</li> <li>Power rating</li> </ul>
<b>Diesel Gensets</b>	<ul style="list-style-type: none"> <li>Unit capital cost</li> <li>Fixed operating cost</li> <li>Runtime-dependent operating cost</li> </ul>	<ul style="list-style-type: none"> <li>Fuel consumption curve</li> <li>Minimum up/down time</li> <li>Start-up time</li> <li>Maximum ramp rate</li> <li>Minimum loading</li> <li>Power rating</li> </ul>



### 3.1.2 Data collection: grid components

**Benefit:** The grid component library allows users to quickly construct models from pre-existing wire elements values without having to conduct extensive data collection.

**Description:** The grid component library contains default values to define topology elements as required by the optimization. These values have been collected from industry sources and have been selected to be representative of elements including overhead and underground lines. A summary of the collected data can be found in Table 3 and Table 4.

*Table 3 - Summary of Grid Component Parameters*

Technology	Operational Parameters	Supplemental Parameters
<b>Overhead Lines</b>	<ul style="list-style-type: none"> <li>Series impedance matrix</li> <li>Shunt impedance matrix</li> <li>Summer rated current</li> <li>Winter rated current</li> <li>Nominal voltage</li> </ul>	<ul style="list-style-type: none"> <li>Phase conductor type</li> <li>Neutral conductor type</li> <li>Conductor spacing</li> <li>Material (if applicable)</li> <li>Line description</li> </ul>
<b>Underground Lines</b>	<ul style="list-style-type: none"> <li>Series impedance matrix</li> <li>Shunt impedance matrix</li> <li>Summer rated current</li> <li>Winter rated current</li> <li>Nominal voltage</li> </ul>	<ul style="list-style-type: none"> <li>Cable neutral type</li> <li>Cable outer diameter</li> <li>Cable phase conductor</li> <li>Cable strand conductor (if applicable)</li> <li>Cable number of neutral strands (if applicable)</li> <li>Cable dielectric relative permittivity</li> <li>Cable spacing</li> <li>Material (if applicable)</li> <li>Line description</li> </ul>

*Table 4 - Summary of Grid Components*

Technology	Phasing	Count	Ampacity
<b>Overhead Line</b>	Three-Phase Neutral	8	120 A
	Three-Phase without Neutral	8	120 A – 765 A
	Line-Line with Neutral	1	120 A – 765 A
	Line-Neutral	2	120 A – 535 A
<b>Underground Line</b>	Three-Phase Neutral	1	495 A
	Three-Phase without Neutral	1	260 A



### 3.1.3 Component library update

**Benefit:** The component library allows users to quickly construct models from preexisting technology definition values without having to conduct extensive data collection

**Description:** The component library contains default values to define technology models as required by the optimization and will be pre-loaded by default when users create new models. This library is currently organized using JavaScript Object Notation (JSON), a lightweight data-interchange format.

As examples, the corresponding updated datasets of one overhead line and one underground cable represented using JSON schema are shown below. These include descriptive data such as the type of element (overhead or underground), and technical characteristics including self and mutual resistance (R), reactance (X), conductance (G) and susceptance (B):

#### [Typical Overhead Line]

```
oh_3ph_12.47_4/0aac_without_neutral:
  type: oh_line_cfg
  ph_cond: 4/0 AAC - 7 Strand
  neu_cond: NONE
  phasing: ABC
  spacing: oh_3ph_12.47_horiz_underbuilt_geom
  Vrated: 7200.0
  Imax: 475.0
  Imax_winter: 605.0
  description: "OH 3-Ph 12.5/7.2 kV w/o Neutral"
  # units: Ohms/mi
  R:
  - [0.5346, 0.0953, 0.0953]
  - [0.0953, 0.5346, 0.0953]
  - [0.0953, 0.0953, 0.5346]
  # units: Ohms/mi
  X:
  - [1.4659, 0.7944, 0.7103]
  - [0.7944, 1.4659, 0.7944]
  - [0.7103, 0.7944, 1.4659]
  # units: Siemens/mi
  G:
  - [0, 0, 0]
  - [0, 0, 0]
  - [0, 0, 0]
  # units: Siemens/mi
  B:
  - [4.943, -1.425, -0.7747]
  - [-1.425, 4.943, -1.425]
  - [-0.7747, -1.425, 4.943]
```

### [Typical Underground Cable]

```
ug_3ph_30.0_1000cc:  
  type: ug_cable_cfg  
  ph_cond: 1000 CC - 1 Core - 61 Strand - Concentric Neutral - 14 CC - 21 Wire  
  neu_cond: NONE  
  phasing: ABC  
  spacing: ug_3ph_horiz_geom  
  Vrated: 30000.0  
  Imax: 350.0  
  Imax_winter: 350.0  
  description: "UG 3-Ph 30 kV underground cable with concentric neutral"  
  # units: Ohms/mi  
  R:  
  - [0.5209, 0.0953, 0.0953]  
  - [0.0953, 0.5209, 0.0953]  
  - [0.0953, 0.0953, 0.5209]  
  # units: Ohms/mi  
  X:  
  - [1.486, 1.244, 1.244]  
  - [1.244, 1.486, 1.244]  
  - [1.244, 1.244, 1.486]  
  # units: Siemens/mi  
  G:  
  - [0, 0, 0]  
  - [0, 0, 0]  
  - [0, 0, 0]  
  # units: Siemens/mi  
  B:  
  - [192.7, 0, 0]  
  - [0, 192.7, 0]  
  - [0, 0, 192.7]
```

## 3.2 Optimization formulation and Numeric Implementation

### 3.2.1 Stochastic generation formulation

**Benefit:** This feature provides a more comprehensive representation of intermittent renewable output compared to deterministic approaches.

**Description:** Given that output from distributed renewable resources such as wind and PV is intermittent, a deterministic optimization model has some limitations in modeling systems with significant installations of these resources. To address this, the project team has analyzed enhancements to deterministic analysis by exploring alternative formulations to incorporate stochastic renewable sources in the model and evaluate trade-offs in accuracy and run-time in the optimization problem.

In this section, we summarize the progress made with this regard, covering the design and operation of off-grid microgrids under wind uncertainty.



- Uncertainty contributed by wind sources can be modeled via random variables with known statistics (mean, variance). Based on the existing data and literature<sup>1</sup>, wind uncertainty due to wind can be modeled as a Gaussian distribution.
- Participation of the controllable, conventional generators can be modeled proportional to the wind fluctuations using the affine control law of the form:  $P_i = P\_mean - A_i * W_i$ ,  $A_1 + A_2 + \dots + A_n = 1.0$ , where  $W_i$  represents the wind fluctuation in  $i$ -th wind farm and  $A_i$  represents the participation factor of  $i$ -th conventional generator.
- In the “LinDist” power flow model which accounts for real and reactive flow, the thermal line limit constraints are modeled as probabilistic chance constraints, i.e.,  $\text{Prob}[(p^2 + q^2 \leq T^2)] \geq 1 - \epsilon$ , where  $\epsilon$  is a specified small number. Intuitively, this constraint implies that the prescribed line limit may be violated during surplus wind injections, but limited to shorter durations, which is controlled using the  $\epsilon$  parameter. Constraint of this form falls under the category of untractability which cannot be simplified via trivial approximations. Hence, we apply conservative, convex inner approximations of the chance constrained set to solve the problem efficiently<sup>2</sup>.
- Testing on wind sources with various statistical characteristics seem to suggest the following:
  - If the power injected due to wind sources is in surplus and greater than the total demand, as expected, the optimization methodology suggests building additional storage devices like batteries.
  - The probability of the risk of failure of network components like generators and lines are decreased considerably when the stochastic model is compared with its deterministic counterpart.
  - Out-of-distribution testing, such as with Weibull and biased-Normal distributions, suggest that the violation probabilities of network components are not increased. This is further an indication of correctness of the initial assumption on Gaussian requirements.

### 3.2.2 Chance constrained formulation and implementation

**Benefit:** This feature provides a fast and accurate method to account for intermittent renewable output

**Description:** Chance constraint formulations are one of the major approaches used to solve optimization problems where different sources of uncertainty may occur. By definition, a chance constraint is used to ensure that the probability of meeting a certain constraint is above a certain level, thus restricting the feasible region so that there is a high confidence level in the solution. In this case, we developed a chance constrained formulation to incorporate the variability in wind generation in the optimization problem, as detailed in Section 4.1 (Annex).

---

<sup>1</sup> Sundar, K., Nagarajan, H., Lubin, M., Roald, L., Misra, S., Bent, R. and Bienstock, D., 2016, June. Unit commitment with n-1 security and wind uncertainty. In Power Systems Computation Conference (PSCC), 2016 (pp. 1-7). IEEE.

<sup>2</sup> Lubin, M., Bienstock, D. and Vielma, J.P., 2015. Two-sided linear chance constraints and extensions. arXiv preprint arXiv:1507.01995.



### 3.2.3 Network design formulation and implementation

**Benefit:** Rather than relying on user-defined networks only, the tool will be able to optimally size and configure the topology to the electrical and thermal network.

**Description:** In the formulation implemented during Phase 2, the topology and capacities of the network branches are treated as decision variables within the optimization, allowing the network structure to be optimized. These capabilities allow extending significantly the applications of the tool to microgrid design, as the topology itself becomes part of the decision variables, in addition to the optimal sizing, placement, and dispatch.

Here, we summarize the solution implemented to achieve the optimal design, planning and operation of N-1 secured, resilient off-grid microgrids with focus on the design of topology or the interconnections between the buses.

- The optimal topology design of microgrids is an NP-hard problem, whose complexity becomes even harder with operation over an extended period. In the literature, there has been progress to solve the problem by decomposing in to smaller time periods without guarantees on the quality and feasibility of solutions. Hence, we apply a modified rolling/receding horizon (RH) algorithm, which is briefly described in Figure 1. The main idea of this approach is to maintain a control and a predictive horizon, where “control horizon” evaluates the solutions of the control variables in the current time period and the “predictive horizon” incorporates the future-time information to improve the control horizon solutions. This approach is iteratively applied by marching in time.

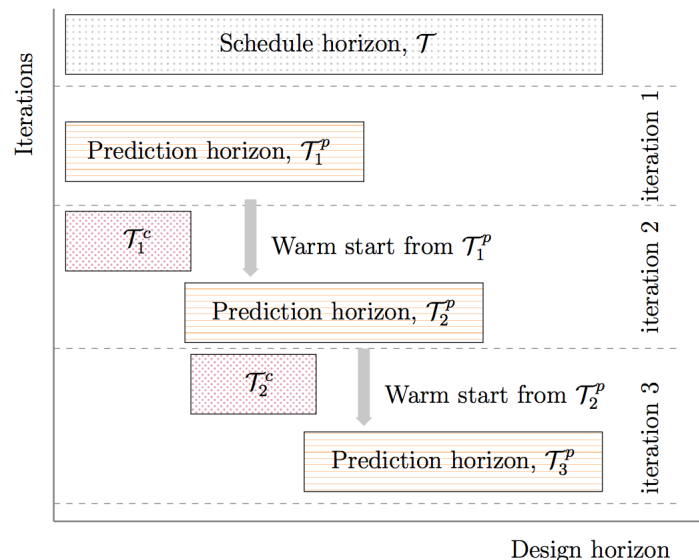


Figure 1 Schematic diagram for rolling horizon



- Compared the efficiency of RH algorithm with scenario-based decomposition (SBD) algorithm which was developed in our earlier work primarily to handle the complexity of N-1 security constraints<sup>3</sup>.
- As a natural extension, based on the computational advantages of RH and SBD algorithms, we developed a hybrid algorithm (SBD-RH) that combines SBD to handle N-1 security constraints at every iteration of RH for a given time stage.
- Numerically, we tested SBD-RH algorithm on IEEE 13 and Nome (Alaska) case studies as shown in Figures 2 and 3, respectively. We observed that the proposed SBD-RH algorithm faster than other methods by orders of magnitude, particularly on instances with larger time steps (up to one day). On the Alaskan grid, though SBD-RH performed well, basic RH was faster in comparison since the instance did not exhibit dominant scenarios and all the N-1 security constraints were binding.

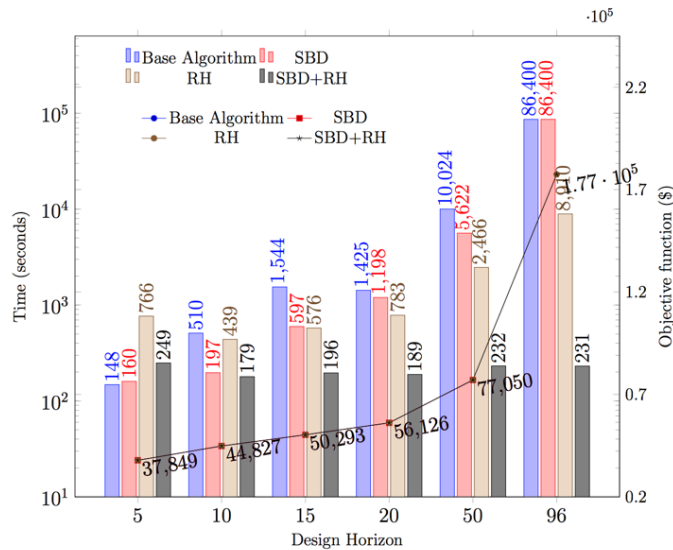


Figure 2 Solution times and solution quality for the IEEE 13 case

<sup>3</sup> Madathil, S.C., Yamangil, E., Nagarajan, H., Barnes, A., Bent, R., Backhaus, S., Mason, S.J., Mashayekh, S. and Stadler, M., 2017. Resilient Off-grid Microgrids: Capacity Planning and N-1 Security. IEEE Transactions on Smart Grid.

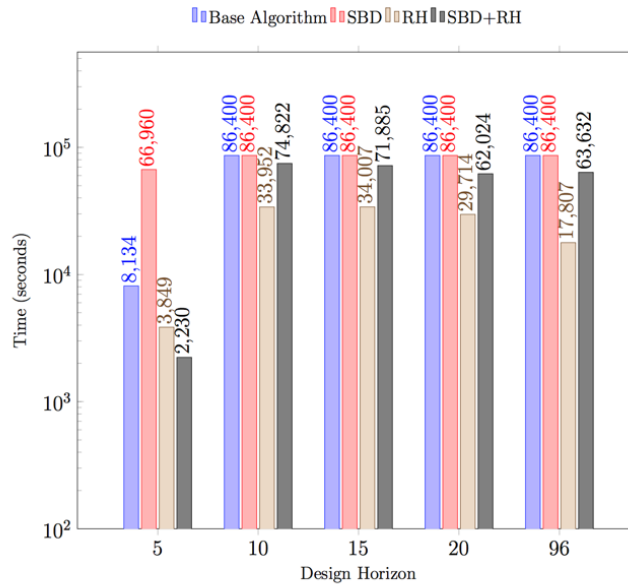


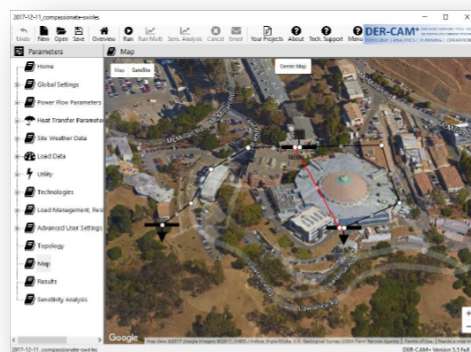
Figure 3 Solution times and solution quality for the Alaskan microgrid case

### 3.3 Network Design and Visualization

#### 3.3.1 GIS Visualization

**Benefit:** This feature enables users to create more realistic visualizations of the microgrids being modeled than using only schematic one-line diagrams.

**Description:** In the work developed through Phase I of this project, we implemented the ability to represent schematic 1-line diagrams of the microgrids under consideration. In Phase II, this was expanded by introducing the ability to create an alternative representation supported by GIS. This allows users to define each of the microgrids nodes over a map using simple latitude and longitude coordinates and draw the respective connections (electric and heating).



## 3.4 Design/Dispatch sensitivity calculations

### 3.4.1 Design sensitivity

**Benefit:** Sensitivity analysis allows users to understand which inputs drive their system designs and to create designs that are more resilient or responsive to possible changes.

**Description:** Through Phase I, we developed the basic procedures and interfaces required for sensitivity analysis. In Phase II, we re-designed this feature in a flexible way to enable any arbitrary sensitivity analysis to be achieved while leveraging the client-server software architecture used by the tool's graphical interface. Particularly, the sensitivity analysis capabilities developed in Phase II rely on the use of newly implemented Representational State Transfer (REST) Application Programming Interface (API) endpoints that enable single requests to trigger multiple optimization jobs and sweep a range of input values (i.e., one request to many results). These requests consist of a "payload", where a set of instructions that establish the sensitivity analysis process is sent to the server in addition to the model data, as illustrated below.

In this example, the "sheet" parameter defines the dataset under analysis, "r0, c0, dr, dc" define the elements to be modified, and "op, snop1, rop1, cop1, opv2" are used to define the modification taking place in a given step of the sensitivity analysis process.

```
"name": "Interest Rate: -2%, -1%, Base Case, +1%, +2%",  
"labels": [ "Base Case", "-2%", "-1%", "+1%", "+2%" ],  
"modificationParam": {  
  "jobs": [  
    {  
      "instructions": [  
        {  
          "sheet": "parameterTable",  
          "r0": 0,  
          "c0": 1,  
          "dr": 0,  
          "dc": 0,  
          "op": "+",  
          "snop1": "parameterTable",  
          "rop1": 0,  
          "cop1": 1,  
          "opv2": -0.02  
        }  
      ]  
    }  
  ]  
},
```

Figure 4 – Example of sensitivity analysis JSON payload

The results of the sensitivity analysis process are fully integrated with the graphical user interface, as illustrated below:

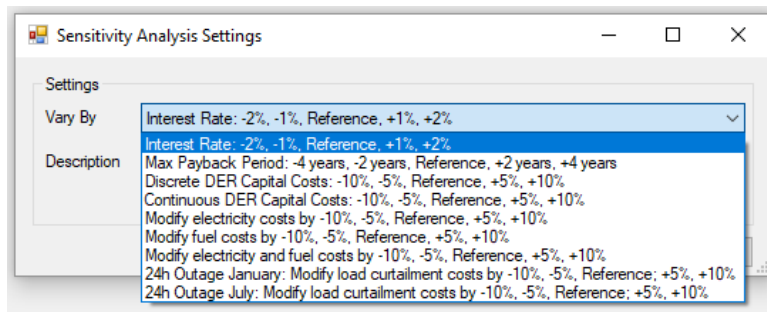


Figure 5 – Example of sensitivity analysis options added to the user interface

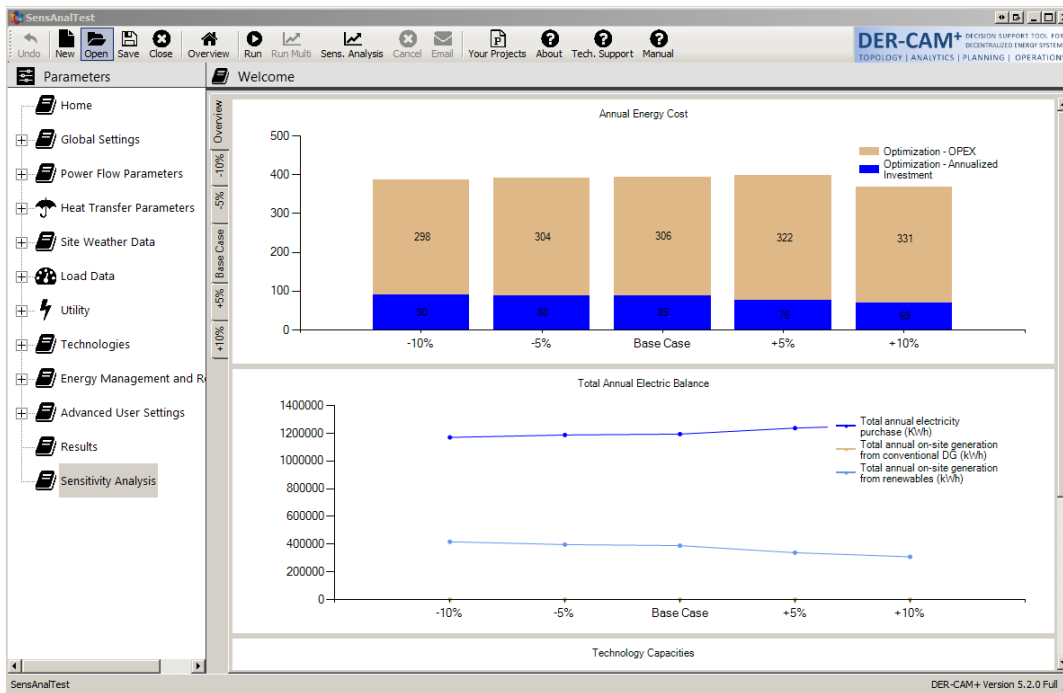


Figure 6 – Example of sensitivity analysis results in the user interface

### 3.5 Tool Testing

#### 3.5.1 Testing against current microgrids – tech mix and operation

**Benefit:** Testing and validation exercises ensure the results obtained from the tool comply with current microgrid practices.

**Description:** Upon completion of tool development and testing, the tool was used to study real-world microgrids. This application allowed showcasing the value of the tool throughout the design process. The results of this activity were used to further promote the tool and expand its market impact. In Phase



I of the project, we focused on the Nome Microgrid. In the second Phase, we have collaborated with our industrial partners to study several microgrids, including the Clarkson Avenue Microgrid, two microgrids in New York State, and the City of Cordova Microgrid.

Some additional details on this task are presented in annex, which is further documented in individual reports prepared with the industrial partners that describe the modeling process, the design and analysis criteria, key results and take-aways, and recommendations for future enhancements and development.

### 3.5.2 Testing against existing design tools

**Benefit:** Evaluates the new tool against the existing tools and methods for microgrid design and highlights the advantages of ROMDST.

**Description:** Although the new tool is unique in terms of its capabilities for designing DC or AC off-grid microgrids, there are alternative tools, such as HOMER, that are currently being used to support the design of such microgrids. Further, different methods, such as heuristic and metaheuristic optimization methods, can also be used for microgrid design. In this task, we compare modeling capabilities and existing microgrid design tools and methods using the same input data and analyze the differences and underlying assumptions leading to different outcomes.

Testing the tool against existing design tools and methods (e.g. HOMER and spreadsheet-based approaches) was done in collaboration with industrial partners and is described in the individual microgrid study reports. In addition to comparisons with standard commercial solutions, we focused in comparing our formulation with other optimization methods, namely meta-heuristics. In particular, we compared our Mixed Integer Linear Programming (MILP) approach with Particle Swarm Optimization, a common meta-heuristic used to solve the problem of optimal sizing and placement of DER in microgrids.

#### *Motivation for the Comparison with Particle Swarm Optimization:*

Three methods are predominantly found in literature to address the problem of Optimal Sizing and Placing of DERs (OSP-DER): analytical, numerical, and heuristic. Analytical methods are typically applied to simplified versions of the problem, e.g. small networks with fixed capacity generation. Numerical methods can be found in many forms, such as gradient search, linear and non-linear programming, exhaustive search, dynamic programming, etc. Among those, MILP solutions, such as DER-CAM, have proven to be very accurate and computationally efficient not only for DG technology selection, sizing and allocation, but also for network expansion. However, the use of heuristics, and metaheuristics in particular, has increased dramatically over the past few years, due to the significant improvements and decreasing costs in the processing power of computers. Within the domain of metaheuristics, Particle Swarm Optimization has become the most popular for different variants of the OSP-DER problem, as it offers solutions to address non-linear formulations within a tractable computational time.

The objective of this analysis is to compare ROMDST with the most popular non-linear approach to optimal design of microgrids, the Particle Swarm Optimization (PSO). This comparison, based on accuracy and computational time, will allow validating and benchmarking the ROMDST solution and its MILP approach.

*Brief description of the method Used*

In PSO, every individual in the swarm, referred to as a particle, represents a candidate solution to the optimization problem, containing a set of possible decision variables. In the microgrid design problem, each particle is composed by a combination of DER investments in the nodes of the microgrid. A fitness function is used to evaluate the position  $x_{ik}$  of individual particles, i.e. the quality of investments, and ultimately to find the optimal solution. Throughout iterations of the problem, each particle tries to improve its position by changing the combination of DER investments. This variation is called “velocity” and is based on the sum of three vectors: (1) the inertia,  $w_i$ , that keeps the direction of changes made in previous iterations; (2) the ability to remember best position of the particle achieved so far (self-memory), known as the personal best position,  $pBest_i$ ; (3) the ability to remember the best position achieved by other particles of the swarm (social memory), known as the global best position,  $gBest_i$ .

$$v_i^{k+1} = v_i^k w^k + c_1 r d_1 (pBest_i - x_i^k) + c_2 r d_2 (gBest_i - x_i^k) \quad \text{Particle velocity}$$

$$x_i^{k+1} = x_i^k + v_i^{k+1} \quad \text{Particles position in each iteration}$$

In the PSO approach, the capacity constraints of DER technologies are included during the process of generating particles (i.e. combination of investments). Although this generation is random, it is possible to force it to consider investments within certain DER capacity limits. In contrast, the constraints associated with the dispatch of technologies are included in the fitness function. An optimal power flow (OPF) is used to solve to hourly dispatch of the DER investments associated with each particle. In case of non-convergence of the OPF, a penalty cost is added to the fitness (cost) of the particle. This penalty is proportional to the number of infeasible hours of the OPF in order to ensure rejection of solutions far from meeting the network constraints, but still keep track of solutions close to the admissible region.

$$fitness(x_i^k) = invCost(x_i^k) + \begin{cases} opCost(x_i^k) & \text{if OPF feasible} \\ Penalty & \text{if OPF infeasible} \end{cases} \quad \text{Fitness Function}$$



In order to compare ROMDST with the PSO method presented above, both approaches were applied to the same microgrid case study and run in the same machine. The network used in this case study was the *Nome Microgrid*. Two ICE generators of 5MW each were assumed to be already installed and ROMDST and PSO methods were applied to an expansion of the DER investments, considering the technologies presented in Table 5.

*Table 5 - DER options portfolio*

DG Technology	Rated Power kW	Lifetime Years	Capital Costs \$/KW	Variable Costs \$/kWh
ICE_LB2500	2500	20	1284	0.232
ICE_LB1000	1000	20	1521	0.257
MT_250	250	15	2311	0.346
ICE_RB_75	75	15	2230	0.3605
PV	-	30	4460	-

As shown in Table 6, the optimal annual costs suggested by ROMDST and PSO methods are very similar. In fact, the PSO solution is only 5% better than ROMDST, a value that is within the optimality gap allowed in the ROMDST solver, which means that the two approaches are equivalent in terms of accuracy.

*Table 6 - Annual costs suggested by each method*

MILP Annual Costs [\$]	PSO Annual Costs [\$]
9,876,470	9,368,174

However, a significant difference was observed in type of solutions provided by the two methods. Specifically, the ROMDST suggested an investment scenario where the PV units are spread throughout the network with a gas generator being added at the end of the feeder in order to compensate periods when the solar irradiation is low. In contrast, PSO suggested a smaller PV capacity and a micro-turbine at the end of the feeder. Due to the lower investments in new DG capacity, the PSO solution requires a higher use of the existing 2x5MW ICE generators. Therefore, although the ROMDST solution requires higher investment costs, the PSO solution entails higher variable costs, as it depends more on gas.

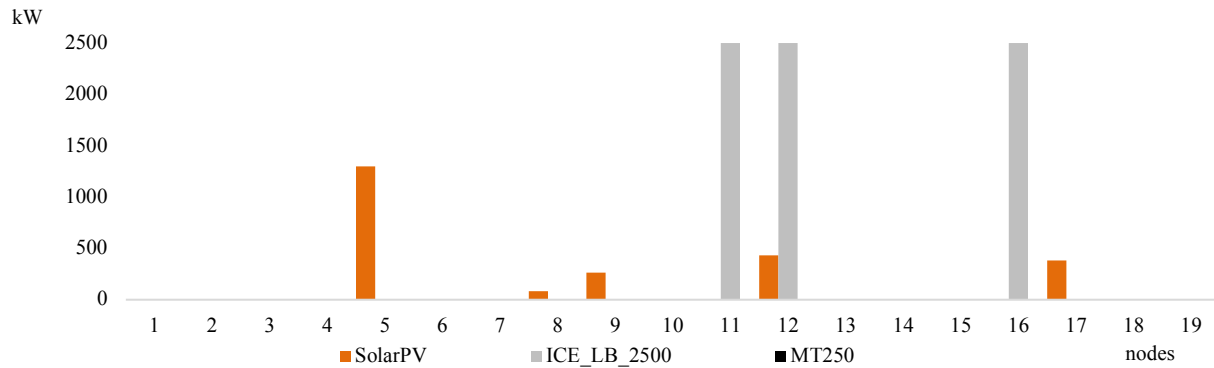


Figure 7 ROMDST Investment Solution

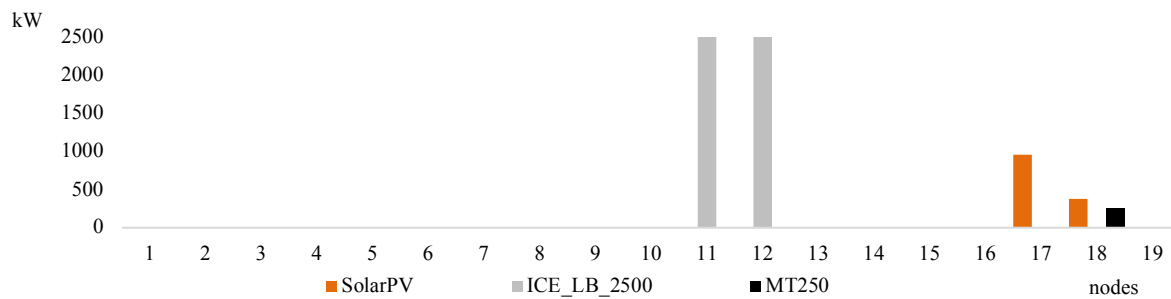


Figure 8 Particle Swarm Optimization Investment Solution

Although the two approaches resulted in similar costs, the ROMDST MILP method was better in terms of computational time. An investment solution was found within 2 hours while the PSO took around 30 hours to run, assuming 30 particles and a maximum number of 80 iterations.

Overall, this analysis validates the use of the MILP approach implemented in this project.

### 3.5.3 Verification against power flow software

**Benefit:** Ensures accuracy of the underlying power flow models in the tool.

**Description:** The power flow equations integrated into the ROMDST formulation are linearized due to the mixed-integer linear form of the ROMDST optimization problem. To evaluate the accuracy of the approximations, we have compared the power flow solution from the optimization with exact power flow solution from GridLAB-D for our studies in the first phase. We have observed good accuracy for the power flow. These studies were continued in the second phase, where we have further evaluated the accuracy of the tool’s results against PYPOWER and MATLAB/Simulink.



PYPOWER is a python implementation of MATPOWER, an open source power flow tool based on the Newton-Raphson method. The ROMDST dispatch solution found in the *Nome Microgrid* case study in Phase I was considered in this analysis.

PYPOWER was run for each hour of the dispatch to check if voltages and line flows were kept within technical limits. After evaluating all 864 hours considered in the yearly analysis done in our model, no ampacity violations were found and only two small voltage violations were observed in the *January Week Profile*, at 10 and 11 pm, and the maximum voltage violation observed was less than 1%, as show in Figure 9.

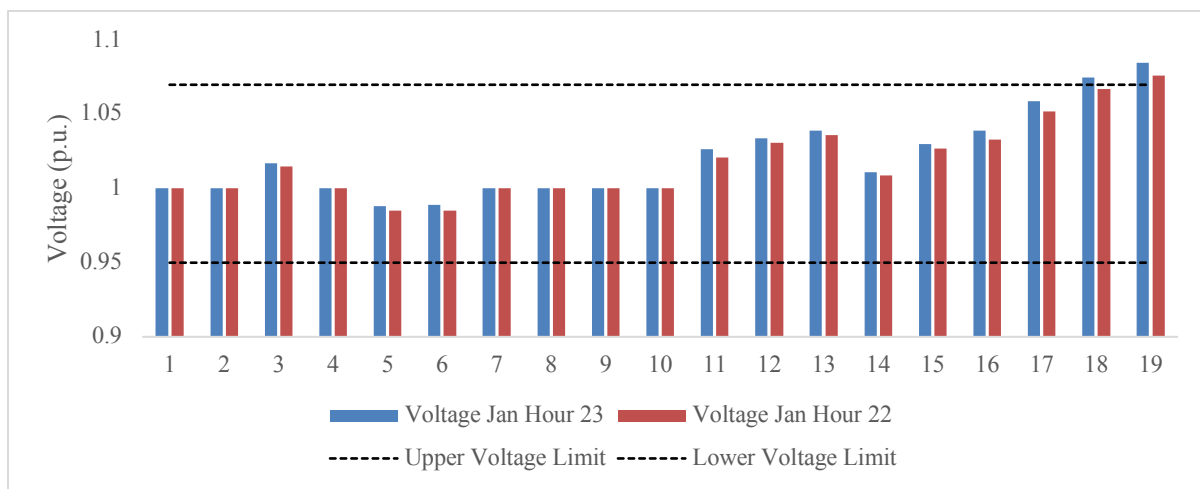


Figure 9 Voltage violation in ROMDST for the critical months when Verified with PYPOWER

In addition to the comparison with PYPOWER, a similar analysis was conducted against MATLAB/Simulink. This solution is often used for detailed modeling and simulation of system dynamics, and also enables steady-state power flow studies.

In this case, the analysis was done using data for the City of Cordova, in Alaska, using hourly data for a year of representative loads (864h), similarly to the discretization used in Phase I.

Again, results obtained using an external power flow solver validate the accuracy of the method implemented in ROMDST, with similar results to those obtained in comparisons with GridLab-D and PYPOWER. This is illustrated below, where the comparison between the voltage magnitude obtained by MATLAB/Simulink and the ROMDST tool is presented for the noon hour in September at each of the buses used to model the City of Cordova Microgrid.



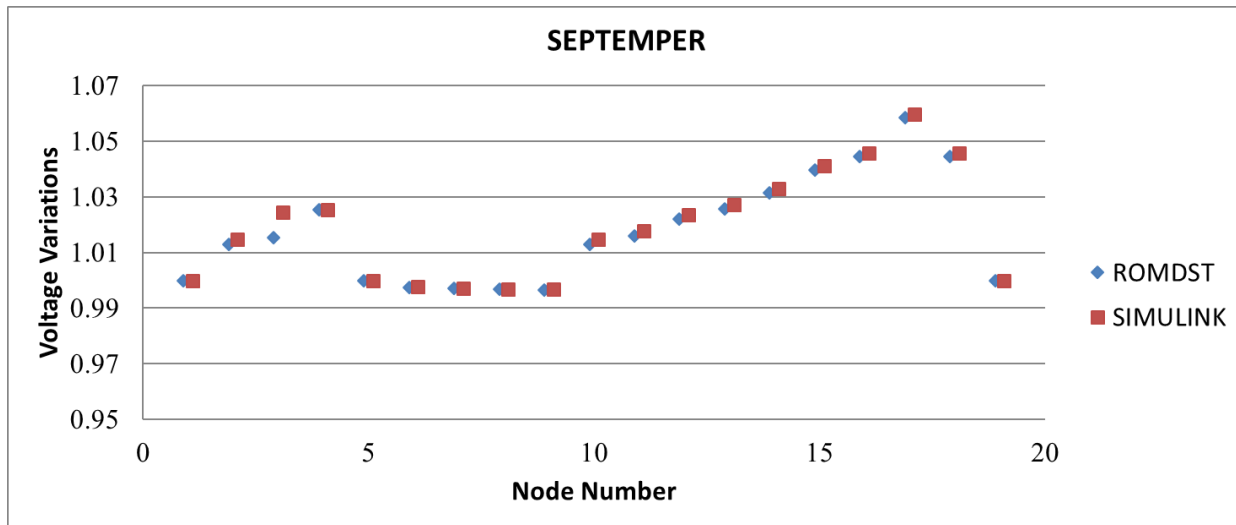


Figure 10 Voltage violation in ROMDST for the critical months when Verified with PYPOWER

### 3.6 Transition to end users

This section describes the transition efforts of the project related to end-user outreach and improvement of documentation to support the use of the tool. Besides this effort, LBNL will keep DER-CAM available and free access in [DER-CAM website](#).

#### 3.6.1 Manual preparation

**Benefit:** Provides users a complete resource of the tool’s use.

**Description:** The user manual was developed in parallel with the development of the tool. It includes all necessary information to operate the tool for a variety of use cases. In addition, each individual input set available in the tool is accompanied by a supporting help file describing the individual parameter and/or intended use for modeling applications.

The full manual can be accessed [here](#).

Lastly, we have developed additional training material detailing the modeling workflow to be followed by users addressing multiple use cases and ownership configurations, which include the remote off-grid applications covered in this project.

The tool workflow video can be seen [here](#) and the workflow presentation can be accessed [here](#).

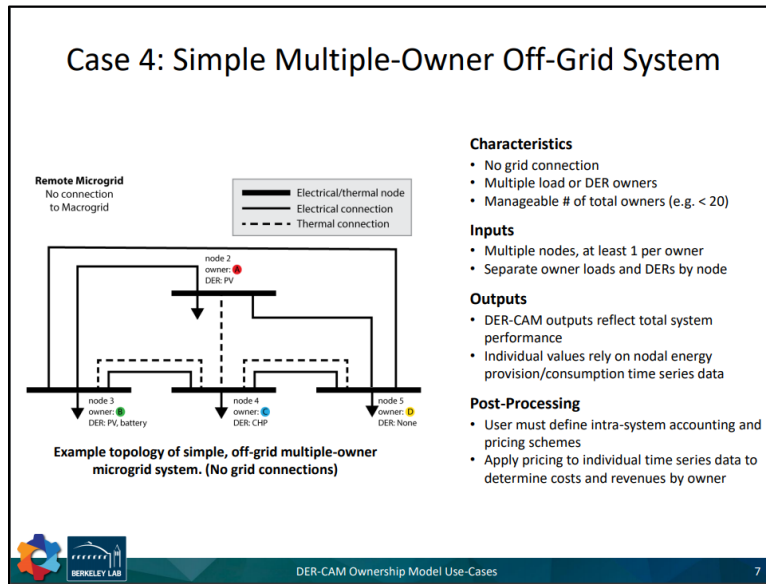


Figure 11 – Example snapshot of documentation describing remote off-grid applications

### 3.6.2 Holding training classes

**Benefit:** Helps in transitioning the tool to its end-users by training them.

**Description:** We held several training classes and workshops in the first phase, during which some of the tool features were presented to the participants and the in-development version of the tool was offered to them for testing purposes. This practice continued in the second phase and online/in-person classes were held according to the planned schedule.

Specifically, the close collaboration between LBNL and the Alaska Center for Energy and Power resulted in two separate training efforts. These consisted of introducing the ROMDST tool in the “Appropriate and Sustainable Engineering” course syllabus at Seattle Pacific University, where it was used to complete course assignments focusing on Alaskan communities as shown in figure 12.

Future workshops can be requested using the following contacts:

Type of Workshop	Institution	Contact
DER-CAM Introduction	Berkeley Lab	dercam@lbl.gov
Alaska Remote Microgrids Modeling	ACEP	gmroe@alaska.edu




## Alaska community analysis

**Required information**

- Community name
- Map coordinates (longitude, latitude, elevation)
- Population
- Topology – map with scale, layout, major sites
- ANCSA regional corporation
- Alaska climatic zone
- Structure inventory estimate
- Power plant data – gensets, electrical rates
- Energy requirement estimates
  - Electrical
  - Space heating & hot water
  - Residential, community, commercial

**Resources (others also acceptable)**

- [AVEC](#)
- [AK Energy Data Gateway](#)
- [AK Division of Community and Regional Affairs](#)



Student	Village
Daniel	Oscarville
Garrett	Katag
Hunter	Minto
Logan	Scammon Bay
Luke	Shishmaref
Nick	Brevig Mission
Sierra	Yakutat
Stephanie	St Marys
Tristan	Mountain Village
Tyler	Wales

Figure 12 - Sample material from the SPU training

In addition, ACEP worked with LBNL to offer a local training workshop as a parallel activity to the 2018 Alaska Rural Energy Conference in Fairbanks. This workshop was attended by representatives from the Alaska Energy Authority, the Fairbanks North Star Borough, and the Alaska Center for Energy & Power, and covered different aspects of the modeling tool developed under this project, as well as multiple Alaska case studies.

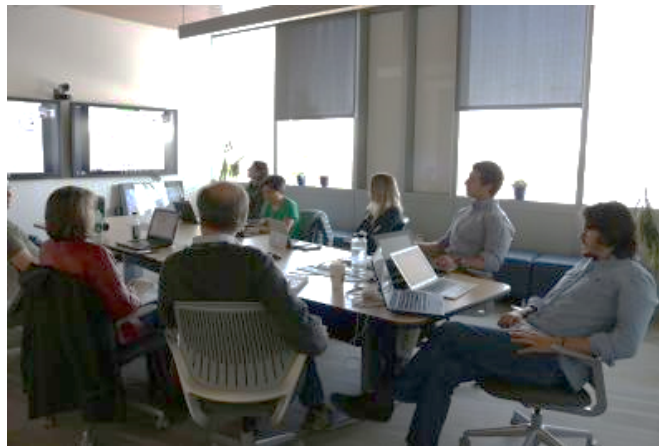


Figure 13 - Training workshop in Fairbanks, AK

The overall feedback from this workshop was very positive and has led to follow-up discussions to draft a scope-of-work for additional training and technical support activities following Phase II of this project. The workshop material can be found in the following links: [Session 1](#); [Session 2](#); [Session 3](#).

Separately to the above efforts, LBNL also participated in the IEEE - Northwest Energy Systems Symposium in Seattle. This event was attended by roughly 130 engineers, utility representatives, researchers, and energy experts, and LBNL's presentation covered the work developed under the ROMDST project. This effort led to engaging with energy consulting experts currently working with the Metlakala community in Alaska, and to follow-up individual training.



*Figure 14 - Microgrid modeling presentation at NWESS 2018*

Finally, outreach and dissemination efforts continued to include other industry and academia interactions as observed throughout the duration of the project. Particularly, the project team at LBNL has organized several 1-on-1 sessions with key project partners and microgrid designers, including GE Energy Consulting, Burns Engineering, and ACEP, which led to continued feedback towards the tool's development (e.g., leading to the inclusion of run-of-river hydro as a generation asset in the model). Additional industry interactions involving the ROMDST tool included in-person, phone, or e-mail assistance to multiple energy consulting firms such as Deloitte, TOTAL Energy, DNV Kema, BRSinv, Lovelady Energy LLC, MicrogridLabs, XENDEE, Exergy Energy (L03 Energy), LaBella Associates, CHA, GI Energy, or Advisian, among others.

Notably, GE Energy Consulting has leveraged the experience gained in this project to become familiarized with the features offered by the tool and has selected it for all its microgrid modeling work in the context of NY Prize. GE Energy Consulting is a partner in 4 out of 11 awardees of the Phase II microgrid studies, representing a total award of \$4M. In addition, Burns Engineering engaged in one additional Phase II NY Prize award, illustrating the strong impact of this project in real-world microgrid deployment efforts.

This successful project collaboration has also led to GE Energy Consulting to expand its internal modeling capabilities using the tool (including experts from GE Power, GE Global Research, and GE Capital) and to



offer independent training to third parties (e.g. National Grid and the Inter-American Development Bank).

### 3.6.3 Other dissemination activities:

Finally, in addition to the preparation of training materials, the outreach and dissemination efforts of this project also contemplated the preparation of several peer-reviewed scientific publications throughout Phases I and II. These contribute to exposing the project to further external scrutiny and validating the methods and solutions developed throughout its duration.

Presented below is the list of scientific publications resulting from work developed in the ROMDST project:

- S. C. Madathil, E. Yamangil, H. Nagarajan, A. Barnes, R. Bent, S. Backhaus, S. J. Mason, S. Mashayekh, M. Stadler, "Resilient Off-grid Microgrids: Capacity Planning and N-1 Security," in IEEE Transactions on Smart Grid, vol. PP, no. 99, pp. 1-1.
- Salman Mashayekh, M. Stadler, G. Cardoso, M. Heleno, S. C. Madathil, H. Nagarajan, R. Bent, M. Mueller-Stoffels, X. Lu, J. Wang, "Security-Constrained Design of Isolated Multi-Energy Microgrids," accepted for publication in IEEE Transactions on Power Systems, 2017.
- Miguel Heleno, Salman Mashayekh, Michael Stadler, Gonçalo Cardoso, and Rodrigo De Luís, "Optimal Sizing and Placement of Distributed Generation: MILP vs PSO Comparison in a Real Microgrid Application," in Proc. Intelligent System Applications to Power Systems (ISAP) Conference, San Antonio, TX, Sep. 2017.
- Hari, S.K.K., Sundar, K., Nagarajan, H., Bent, R. and Backhaus, S., 2018. "Hierarchical Predictive Control Algorithms for Optimal Design and Operation of Microgrids", in Power Systems Computation Conference, Dublin, Ireland. 2018. (arXiv preprint arXiv:1803.06705).
- S. C. Madathil, H. Nagarajan, R. Bent, S. J. Mason, S. D. Eksioglu, M. Lu, "Algorithms for Optimal Topology Design, Placement, Sizing and Operation of Distributed Energy Resources in Resilient Off-grid Microgrids" (arXiv:1806.02298v1 [math.OC] 6 Jun 2018)

### 3.6.4 Outreach plan:

During phase II of ROMDST project, a significant effort was dedicated to transfer knowledge from LBNL to ACEP in order to create a community of DER-CAM users in Alaska, with a special focus in modelling and running microgrid remote planning and investment cases. After this first effort, LBNL will keep maintaining and providing support to the basic DER-CAM functionalities, while ACEP will be available to continue disseminating and supporting Alaska users in modelling real-life microgrid investment problems with the tool.

## 4 Annex – Details on Formulation and Testing

### 4.1 Details on chance constrained formulation

Presented below is the detailed mathematical formulation developed in the Phase II of this project to incorporate uncertainty in wind generator output in the overall optimization problem. This formulation is based on the use of chance constraints and can be generalized to additional sources of uncertainty (e.g. photovoltaics).

**Sets:**

$\mathcal{B}$  - set of buses, indexed by  $b$

$\mathcal{L}$  - set of lines, indexed by  $\ell$

$\mathcal{G}$  - set of generators, indexed by  $i$

$\mathcal{W}$  - set of buses with wind generation

$\mathcal{T}$  - set of discretized times (hours), indexed by  $t$

$\mathcal{C}_g$  - set of generator contingencies, indexed by  $gc$

$\mathcal{C}_\ell$  - set of line contingencies, indexed by  $lc$

**Binary decision variables:**

$x_i(t)$  - generator on-off status at time  $t$

$y_i(t)$  - generator 0-1 start-up status at time  $t$

$z_i(t)$  - generator 0-1 shut-down status at time  $t$

$w_{is}(t)$  - generator 0-1 status if  $i$  starts at time  $t$  after being down for  $s$  hours

**Continuous decision variables:**

$sc_i(t)$  - start-up cost of  $i$  at time  $t$ , \$

$p_i(t)$  - real power output of  $i$  at time  $t$ , MW

$q_i(t)$  - reactive power output of  $i$  at time  $t$ , MVar

$r_i^+(t), r_i^-(t)$  - up-reserve and down-reserve power output of generator  $i$  at time  $t$ , MW

$\alpha_i(t)$  - participation factor of controllable generator  $i$  at time  $t$

$P_\ell(t)$  - real power flow of  $\ell$  at time  $t$ , MW

$Q_\ell(t)$  - reactive power flow of  $\ell$  at time  $t$ , MVar

$\theta_b(t)$  - phase angle at bus  $b$  at time  $t$ ,

$v_b(t)$  - squared voltage magnitude at bus  $b$  at time  $t$ ,

**Parameters:**

$R_\ell, X_\ell$  - Resistance, Reactance of line  $\ell$

$\underline{p}_i, \bar{p}_i$  - minimum and maximum real output of generator  $i$ , MW

$\underline{q}_i, \bar{q}_i$  - minimum and maximum reactive output of generator  $i$ , MVar

$\underline{v}_b$  - squared voltage magnitude's lower bound at bus  $b$ ,

$\bar{v}_b$  - squared voltage magnitude's upper bound at bus  $b$ ,



$d_b^p(t), d_b^q(t)$  - real and reactive power demand at bus  $b$  for hour  $t$ , MW, MVar

$a_{0,i}, a_{1,i}, a_{2,i}$  - cost coefficients of the generator  $i \in \mathcal{G}$

$\bar{S}_\ell$  - thermal capacity of line  $\ell$ , MVA

$\bar{L}_i$  - min. time generator  $i$  has to run, hrs

$\underline{L}_i$  - min. time generator  $i$  has to be off, hrs

$UT_i, DT_i$  - minimum up-time and down-time of generator  $i$ , hrs

$p_i^{\text{up,init}}, p_i^{\text{down,init}}$  - number of time periods generator  $i$  has been on and off before  $t = 0$ ,

$p_i^{\text{on-off}}$  - on-off status of generator  $i$  at  $t = 0$

$p_i(0)$  - power output of generator  $i$  at  $t = 0$ , MW

$RU_i, RD_i$  - ramp-up and ramp-down limit of generator  $i$ , MW/hr

$\mu_b^p(t)$  - real power output of wind farm at  $b$  for time  $t$ , MW

$\mu_b^q(t)$  - reactive power output of wind farm at  $b$  for time  $t$ , MW

$\omega_b(t)$  - actual wind deviations from forecast  $\mu_b(t)$ , at time  $t$

$r$  - index of the reference bus

$R^g$  - bounds on the reserves that can be purchased, MW

### Objective function

$$\min \sum_{i \in \mathcal{G}} \sum_{t \in \mathcal{T}} \{a_{0,i} \cdot x_i(t) + a_{1,i} p_i(t) + a_{2,i} p_i^2(t)\}$$

### Power flow constraints

$$p_b(t) + \mu_b^p(t) - d_b^p(t) = \sum_{l \in \mathcal{E}_b^+} P_l(t) - \sum_{l \in \mathcal{E}_b^-} P_l(t) \quad \forall b \in \mathcal{B}, t \in \mathcal{T}$$

$$q_b(t) + \mu_b^q(t) - d_b^q(t) = \sum_{l \in \mathcal{E}_b^+} Q_l(t) - \sum_{l \in \mathcal{E}_b^-} Q_l(t) \quad \forall b \in \mathcal{B}, t \in \mathcal{T}$$

$$v_j(t) = v_i(t) - 2(R_l P_l(t) + X_l Q_l(t)) \quad \forall l = (i, j) \in \mathcal{L}, t \in \mathcal{T}$$

$$(P_l(t))^2 + (Q_l(t))^2 \leq (\bar{S}_l)^2 \quad \forall l \in \mathcal{L}, t \in \mathcal{T}$$

$$\Pr(\mathbf{v}_b(t) \leq \bar{\mathbf{v}}_b) > 1 - \varepsilon_b \quad \forall b \in \mathcal{B}, t \in \mathcal{T},$$

$$\Pr(\mathbf{v}_b(t) \geq \underline{\mathbf{v}}_b) > 1 - \varepsilon_b \quad \forall b \in \mathcal{B}, t \in \mathcal{T},$$

The above power flow constraints are based on the LinDist flow constraints, as proposed for radial networks. Further, since voltage limits are typically the binding constraints in microgrids, chance-constrained modeling is applied only on voltage-regulation constraints.





### Generator commitment constraints

$$\begin{aligned}
y_i(t) - z_i(t) &= x_i(t) - x_i(t-1) \quad \forall t \in \mathcal{T}, i \in \mathcal{G}, \\
y_i(t) + z_i(t) &\leq 1 \quad \forall t \in \mathcal{T}, i \in \mathcal{G}. \\
x_i(t) &= p_i^{\text{on-off}} \quad \forall i \in \mathcal{G}, t \leq \bar{L}_i + \underline{L}_i, \\
\sum_{n=\bar{t}}^t y_i(n) &\leq x_i(t) \quad \forall i \in \mathcal{G}, t \geq \bar{L}_i, \bar{t} = t - UT_i + 1, \\
\sum_{n=\underline{t}}^t z_i(n) &\leq 1 - x_i(t) \quad \forall i \in \mathcal{G}, t \geq \underline{L}_i, \underline{t} = t - DT_i + 1, \\
RD_i &\geq p_i(t-1) - p_i(t) \quad \forall i \in \mathcal{G}, t \in \mathcal{T}, \\
RU_i &\geq p_i(t) - p_i(t-1) \quad \forall i \in \mathcal{G}, t \in \mathcal{T}.
\end{aligned}$$

Since secure operation of the power system requires balance between produced and consumed power at all times, any deviation must be balanced by an adjustment in the controllable generation. We model these adjustments through an affine policy, reflecting automatic generation control (AGC):

$$p_i(t) = p_i(t) - \alpha_i(t)\Omega(t)$$

Here,  $\alpha_i(t) \geq 0$  is the participation factor for the controllable generator  $i$ . When  $\sum_i \alpha_i(t) = 1$ , the balance of generation and load is guaranteed for every time period  $t$ .

### Generator limits

$$\begin{aligned}
\sum_{i \in \mathcal{G}} \alpha_i(t) &= 1, \quad \alpha_r(t) = 0 \quad \forall t \in \mathcal{T}, \\
0 &\leq r_i^+(t) \leq R^g \cdot x_i(t) \quad \forall i \in \mathcal{G}, t \in \mathcal{T}, \\
0 &\leq r_i^-(t) \leq R^g \cdot x_i(t) \quad \forall i \in \mathcal{G}, t \in \mathcal{T}, \\
p_i(t) - r_i^-(t) &\geq \underline{p}_i \cdot x_i(t) \quad \forall i \in \mathcal{G}, t \in \mathcal{T}, \\
p_i(t) + r_i^+(t) &\leq \bar{p}_i \cdot x_i(t) \quad \forall i \in \mathcal{G}, t \in \mathcal{T}, \\
\Pr(r_i^-(t) \geq \Omega(t)\alpha_i(t)) &\geq 1 - \varepsilon_i \quad \forall i \in \mathcal{G}, t \in \mathcal{T}, \\
\Pr(r_i^+(t) \geq -\Omega(t)\alpha_i(t)) &\geq 1 - \varepsilon_i \quad \forall i \in \mathcal{G}, t \in \mathcal{T}, \\
0 &\leq \alpha_i(t) \leq x_i(t) \quad \forall i \in \mathcal{G}, t \in \mathcal{T}.
\end{aligned}$$

The chance constraints presented above are often non-convex and intractable. But, under the assumption that  $[P_l(t), Q_l(t)]$  is the image, under affine transform, of a random vector  $\mu^p(t)$  with the rotationally invariant distribution (such as the multivariate Gaussian distribution), these equations can be reformulated to a convex form that is computationally tractable. In particular, if  $\xi$  is any multi-variate normal random variable with mean  $\mu$  and covariance matrix  $\Sigma$ , and if  $\xi$  is the decision variable vector, then a chance constraint of the form



$$\Pr(\xi^T v \leq b) \geq 1 - \varepsilon$$

is equivalent to

$$\mu^T v + \phi^{-1}(1 - \varepsilon) \sqrt{v^T \Sigma v} \leq b$$

Here,  $\phi^{-1}$  denotes the inverse cumulative distribution function of the standard normal distribution. The resulting constraint is a convex second-order cone constraint.

## 4.2 Details on microgrid testing

In phase II of the project, an important goal is to perform testing of the ROMDST tool and conduct verification of the results. Although the original intent was to consider 2 microgrids, the research team and industrial partners have been able to identify a total of 4 microgrids to model and test. During this progress period, data collection from all 4 microgrids was completed and the modeling and testing conducted. In this section we present a brief summary of the 4 microgrids, including results from using the ROMDST tool. At the request of the sites, two of the microgrid locations are omitted to address data privacy concerns.

### #1: Clarkson Ave Microgrid

The analysis of Microgrid #1 was conducted in close cooperation with the Burns Engineering Group. Presented below is a summary of the modeling and testing efforts.

Situated in the heart of Brooklyn, New York, the Clarkson Ave Microgrid was a Stage One NY Prize award recipient, winning for its attractiveness as technical feasible and economically viable.

Within this microgrid, the facilities include the following critical loads:

- Kingsboro Psychiatric Center
- State University of New York (SUNY) Downstate Medical Center, and
- Kings County Hospital Center (KCH).

The microgrid will consist of a combination of distributed energy resources (DERs) on local facility campuses and a hybrid resource center. Renewable energy in the form of PV and ultra-low carbon emitting fuel cells as well as CHP are planned to be installed locally to reduce base load of each facility. Due to space constraints at both SUNY Downstate and Kings County (KCH), a Hybrid Energy Resource Center (HERC) with natural gas generators and battery storage systems or other resources will be located on Kingsboro (OMH) to provide the function of load following or peak load reduction for the three campuses with paralleling operation with utility of Con Edison. During emergency or the loss of utility services, the distributed energy resources (DERs) on local campuses and HERC can continuously support the total critical loads of the three facilities as islanding operation at least two weeks. The three facilities and HERC will be connected by 27KV underground distribution power cables (see figure below of the site plan).

The modeling of the Clarkson Ave Microgrid using the ROMDST tool consisted of representing multiple nodes at both the local facility campuses and HERC. An initial model comparison with one node versus multiple nodes indicated the need for multiple node consideration due to differences in DG investment options and operations. The results of the model runs indicated the value of the N-1 generator



contingency constraint functionality in the tool as a means for correctly selecting suitable generator assets and corresponding dispatch to support the microgrid’s islanding operation even during generator failure. The results obtained using the ROMDST tool assist to determine technologies, numbers and sizes of DERs at HERC. Since some DERs of local facilities have been specified and under construction, the results of ROMDST provide references of DERs’ operations and options for future DERs’ installation as well as provide an evaluation method for existing DERs’ selection.

Clarkson Ave Microgrid is modeled as five (5) nodes network system (see Figure 2):

- Node 1 to Node 3 presenting three facilities individually, serving as PQ Load Buses
- Note 4 presenting utility services to three facilities, serving as Slack Bus
- Node 5 presenting Hybrid Energy Resource Center, serving as PV Generator Bus

The three facilities have their own services. Since the ROMDST cannot explicitly model competing optimization objectives that would be associated with each individual facility, all utility services are combined on one node and connected to corresponding load buses with very short power cables in the model.



Figure 15 – Clarkson Ave Microgrid Site Plan

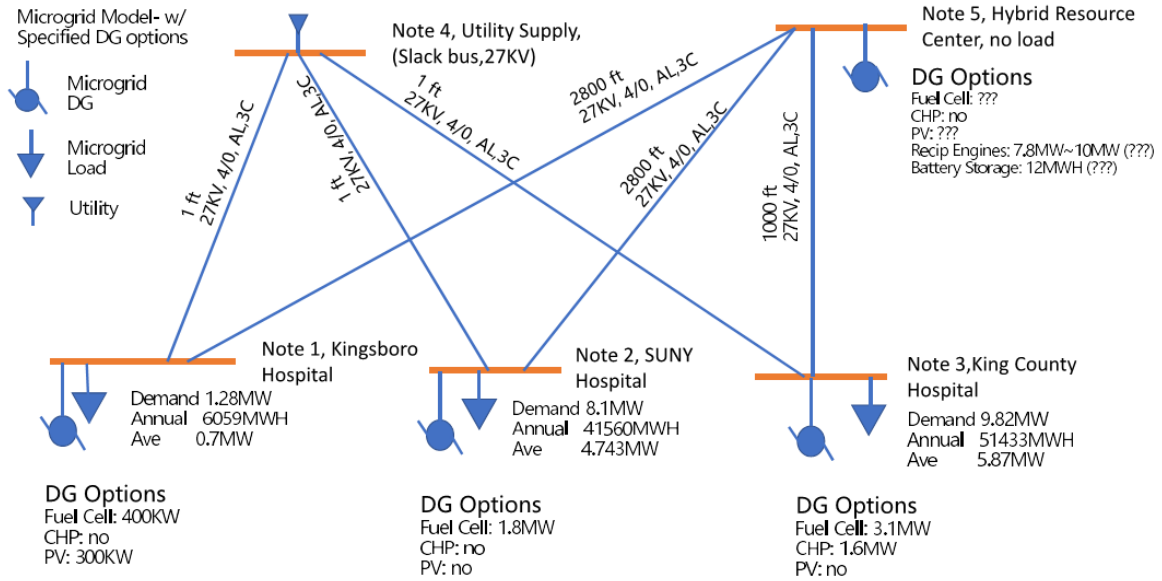


Figure 16 – Clarkson Ave Microgrid ROSMT multi-nodes simulation Model

## #2: Microgrid A

The analysis of Microgrid #2 was prepared in collaboration with GE – Energy Consulting. Due to client privacy concerns, the exact names and facility locations have been anonymized. Below we present a summary of the modeling and testing efforts.

Situated in the New York State Capital region, Microgrid A was chosen because of its attractiveness as a non-wire alternative (NWA) in a location with forecasted high load growth with limited import capabilities as a result of constraints in the upstream transmission system. Microgrid A will consist of a mix of above ground and underground primary distribution feeders for power and communications, interconnecting all the microgrid facilities including all the critical loads and existing and new generation resources. Parts of the Microgrid A network will include some of the existing utility feeders.

Within this microgrid, the facilities include the following critical loads:

- Psychiatric Center
- Law School
- College of Pharmacy
- Nursing Home
- Synagogue.

This microgrid also includes thermal (heating and cooling) loads. In addition to some of the existing backup generators, the microgrid will also include a number of new CHPs, new solar PV installations, a number of electric storage systems, and also a fuel cell. An energy audit has determined the amount of energy efficiency and demand response resources in the microgrid. Actual operation of this microgrid will have to be managed properly in order to achieve certain required combined electrical and thermal efficiencies in order for the microgrid DER to be qualified for additional state incentives.

Total peak load of Microgrid A is about 5,600 kW. Additional new DER needed for resiliency above and beyond the selected existing backup generation and the planned new solar PV and energy storage was determined to be about 2,400 kW of CHPs sited at different locations. Additional model runs will be performed to further improve the microgrid design. The figure below presents the topology of Microgrid A as prepared using the tool's interface. As can be seen, two of the facilities, in addition to be connected by the microgrid electrical network, are also connected thermally through a thermal conduit, and therefore, a CHP in one facility can provide heating to both facilities.



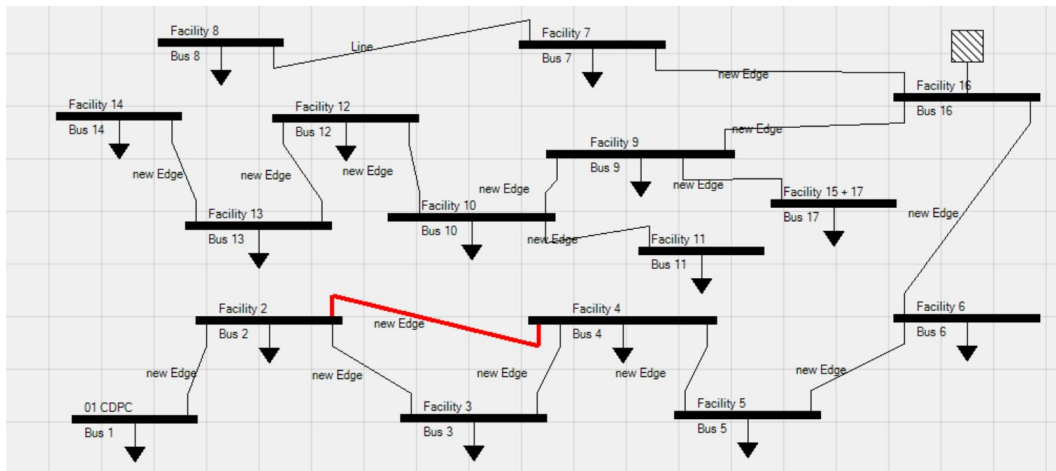


Figure 17 – Topology of Microgrid A represented in the ROMDST tool

In addition to the existing generation assets of about total 2,735 kW capacity, the original amount of additional DER before application of the ROMDST tool included 2,750 kW of combined CHP and electric only units and 1950 kW of solar PV and a 2000 kWh / 1000 kW battery storage. Some of these DER assets were selected to meet certain type and efficiency requirements in order to qualify for state based incentives. However, further analysis using ROMDST considering multiple nodes resulted in a more refined selection of additional 2,360 kW of combined CHP and electric only units and 1,917 kW of solar PV, while also keeping the 2000 kWh /1000 kW battery storage. The following figure provides a view of the microgrid generation and load profile, including power purchase from the grid in a typical weekday in September.

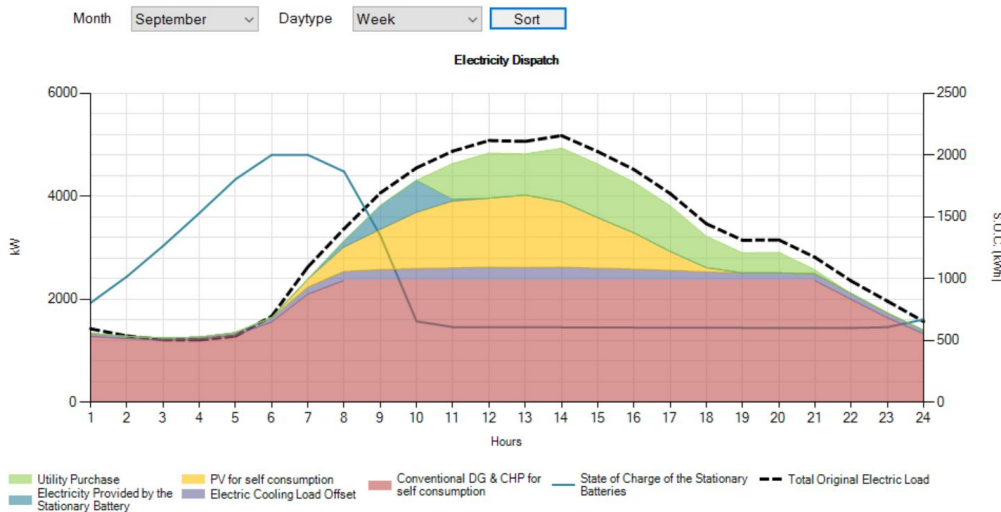


Figure 18 –Electricity Dispatch Profile in a Weekday in September for Microgrid A

### #3: Microgrid B

The analysis of Microgrid #3 was prepared in collaboration with GE – Energy Consulting. Due to client privacy concerns, the exact names and facility locations have been anonymized. Below we present a summary of the modeling and testing efforts.

Microgrid B is located in upstate New York and was chosen because the area is subject to winter ice storms and is susceptible to prolonged power interruptions. The design will include a new underground primary distribution loop for power and communications, interconnecting all the microgrid facilities listed above, including all the critical loads and existing and new generation resources.

The loop will connect the critical loads in the community and will connect at three points to the utility overhead primary distribution system. When islanded operation is required, the underground system will separate from the overhead to carry only the connected emergency service providers. This underground loop will provide the necessary reliability and integrity of primary distribution system required of the microgrid.

Within this microgrid, the facilities include the following critical loads:

- University Campus
- Convenience Store and Gas Station
- Pharmacy
- Water Treatment Plant
- Grocery Store
- Town Civic Center and Village Offices (including Police and Fire stations)
- Hospital
- High School

The microgrid facilities contain several existing backup generations and a grid-scale solar PV power plant and two run-of the river hydropower plants. However, only one of the hydropower plants will be physically connected to the microgrid, but the other two renewable resources will only be part of the financial structure of the microgrids. The analysis also included accounting for year-round energy efficiency.

This microgrid did not include any thermal loads, and hence, the additional new DER selected is about 3000 kW of reciprocating electric engines to be located at the University Campus. Additional model runs will be performed to further improve the microgrid design.

The following figure presents the topology of Microgrid B represented in the ROMDST tool.



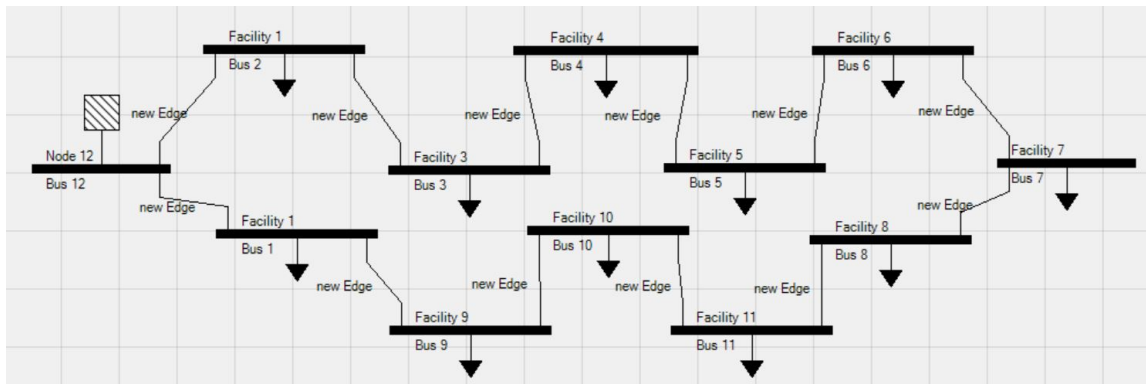


Figure 19 – Topology of Microgrid B represented in the ROMDST tool

Modeling of this microgrid included numerous runs based on various improvements in data and refinements on the sizing of electrical generation units in addition to the selected existing backup generation that are planned to be included in the microgrid network. For instance, two of the scenarios analyzed included a case where new generation sizes were limited to 100 kW, and another case where larger generation units were allowed. Larger units are more efficient and have a lower capital cost on a per kW basis. The table below presents the economic choices determined using the ROMDST tool under the two cases.

Table 7. Results of Two Case Runs for Microgrid B

Microgrid DERs	Unit Size (kW)	Number of Units	Total Capacity (kW)
<b>Case 1</b>			
RECIP – 100 kW	100	29	2,900
Total			2,900
<b>Case 2</b>			
RECIP – 1000 kW	2,000	1	2,000
RECIP – 2000 kW	1,000	1	1,000
Total			3,000

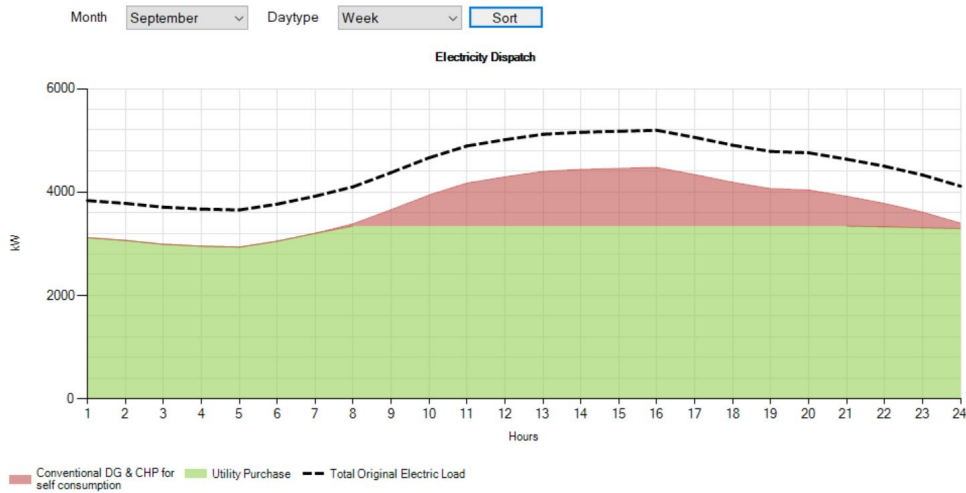


Figure 20 –Electricity Dispatch Profile in a Weekday in September for Microgrid B

#### #4: Cordova Microgrid

The analysis of Microgrid #4 was prepared in collaboration with the Alaska Center for Energy and Power. Due to data privacy concerns, some commercial and industrial load data were aggregated. Below we present a summary of the modeling and testing efforts.

The City of Cordova has a population of more than 2000 people in Alaska. The community is remotely located and hence, is not connected to a macro-grid. The electrical system in Cordova is operated by the Cordova Electric Cooperative. Through the collaboration with Alaska Center for Energy and Power (ACEP), we have accessed high resolution load and operation data.

To represent the City of Cordova topology using the tool’s interface, our team has worked closely with the above partners to collect and treat topology data, load data, and generation data. This exercise lead to building a reduced 19-node model using the tool’s interface, as illustrated below.

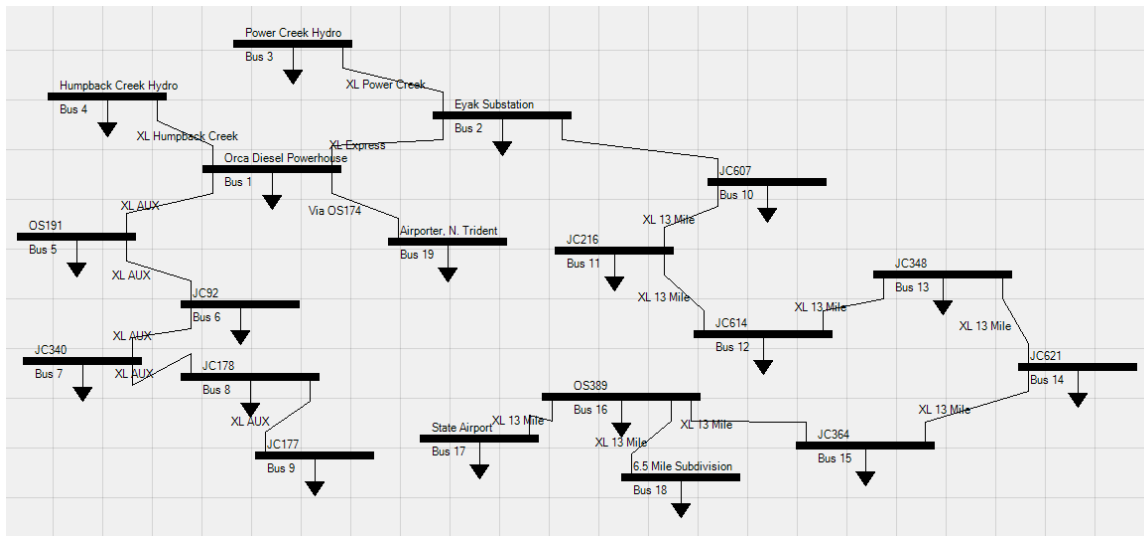


Figure 21 – Topology of Cordova represented in the tool's user interface.

Within this model, several critical and non-critical infrastructures are represented, including multiple residential areas, the local state airport, and different commercial and industrial loads (e.g. local canneries).

In addition, existing generation resources are also represented, including both hydro (4.8 MW) and diesel generation (8.9 MW).

Based on the interactions with local representatives, our analysis focused on the possibility of adding grid-level storage at the Eyak Substation, as well as deploying PV near the State Airport.

Preliminary results obtained with the tool suggest that deploying a total of 4MW of PV by the airport is economically attractive and leads to improving overall voltage conditions in the circuit.

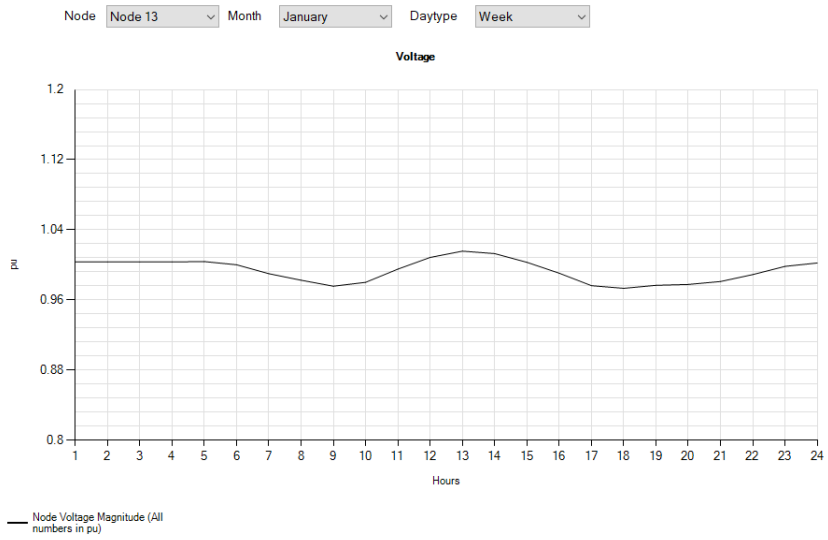


Figure 22 – Example of a voltage profile obtained in the Cordova model.

**Lawrence Berkeley National Laboratory**

One Cyclotron Road | Berkeley, California 94720